

Chemical vapour deposition (CVD) of nickel oxide using the novel nickel dialkylaminoalkoxide precursor [Ni(dmamp')₂] (dmamp' = 2-dimethylamino-2-methyl-1-propanolate)

Rachel L. Wilson¹, Thomas J. Macdonald^{1,2}, Chieh-Ting Lin³, Shengda Xu³, Alaric Taylor⁴, Caroline E. Knapp¹, Stefan Guldin⁴, Martyn A. McLachlan³, Claire J. Carmalt^{1}, Chris S. Blackman^{1,5*}*

Table S1 outlines the crystal data and structure refinement details, and **Table S2** selected bond lengths and bond angles, for [Ni(dmamp')₂].

Table S1: Crystal data and structure refinement for [Ni(dmamp')₂]

| | |
|--------------------------------------|---|
| Empirical formula | C ₁₂ H ₂₈ N ₂ NiO ₂ |
| Formula weight | 291.07 |
| Temperature/K | 150.5(7) |
| Crystal system | orthorhombic |
| Space group | Pbca |
| a/Å | 7.29170(10) |
| b/Å | 10.68490(10) |
| c/Å | 17.7929(2) |
| α/° | 90 |
| β/° | 90 |
| γ/° | 90 |
| Volume/Å ³ | 1386.26(3) |
| Z | 4 |
| ρ _{calc} /g/cm ³ | 1.395 |
| μ/mm ⁻¹ | 1.965 |
| F(000) | 632.0 |
| Crystal size/mm ³ | 0.141 × 0.128 × 0.064 |
| Radiation | CuKα (λ = 1.54184) |
| 2θ range for data collection/° | 15.714 to 148.974 |
| Index ranges | -8 ≤ h ≤ 9, -13 ≤ k ≤ 13, -22 ≤ l ≤ 22 |
| Reflections collected | 19513 |
| Independent reflections | 1410 [R _{int} = 0.0227, R _{sigma} = 0.0078] |
| Data/restraints/parameters | 1410/0/135 |
| Goodness-of-fit on F ² | 1.094 |
| Final R indexes [I ≥ 2σ (I)] | R ₁ = 0.0209, wR ₂ = 0.0566 |
| Final R indexes [all data] | R ₁ = 0.0224, wR ₂ = 0.0582 |

Table S2: Selected bond lengths and bond angles for compound (1) [Ni(dmamp')₂] (in which ¹1-X,1-Y,1-Z).

| Atom - Atom | Length (Å) | Atom - Atom | Length (Å) |
|---|------------|---------------------|------------|
| Ni(1) – O(1) | 1.8427(7) | N(1) – C(1) | 1.5239(12) |
| Ni(1) – O(1) ¹ | 1.8427(7) | N(1) – C(5) | 1.4788(13) |
| Ni(1) – N(1) ¹ | 1.9545(8) | C(3) – C(1) | 1.5319(14) |
| Ni(1) – N(1) | 1.9546(8) | C(4) – C(1) | 1.5311(14) |
| O(1) – C(2) | 1.3992(12) | C(1) – C(2) | 1.5313(14) |
| N(1) – C(6) | 1.4896(13) | | |
| Atom – Atom - Atom | Angle (°) | Atom – Atom - Atom | Angle (°) |
| O(1) – Ni(1) – O(1) ¹ | 180.00 | C(5) – N(1) – Ni(1) | 113.89(7) |
| O(1) ¹ – Ni(1) – N(1) ¹ | 88.43(3) | C(5) – N(1) – C(6) | 106.95(8) |
| O(1) – Ni(1) – N(1) | 88.43(3) | C(5) – N(1) – C(1) | 112.91(8) |
| O(1) ¹ – Ni(1) – N(1) | 91.57(3) | N(1) – C(1) – C(3) | 108.98(8) |
| O(1) – Ni(1) – N(1) ¹ | 91.57(3) | N(1) – C(1) – C(4) | 113.07(8) |
| N(1) – Ni(1) – N(1) ¹ | 180.0(5) | N(1) – C(1) – C(2) | 104.13(8) |
| C(2) – O(1) – Ni(1) | 112.10(6) | C(3) – C(1) – C(4) | 110.37(9) |
| C(6) – N(1) – Ni(1) | 105.98(6) | C(2) – C(1) – C(3) | 108.84(8) |
| C(6) – N(1) – C(1) | 112.61(8) | C(2) – C(1) – C(4) | 111.22(8) |
| C(1) – N(1) – Ni(1) | 104.41(6) | O(1) – C(2) – C(1) | 110.15(8) |

Film thickness was obtained from the ellipsometry measurements and showed an approximately linear relationship of increasing film thickness with deposition temperature (Table S3).

Table S3: Film thickness and refractive index values of NiO films deposited by CVD of [Ni(dmamp')₂] at various temperatures

| Deposition time (hours) | Growth temp (°C) | Film thickness (nm) | <i>n</i> @ 632.8 nm |
|-------------------------|------------------|---------------------|---------------------|
| 24 | 250 | 17 | 1.5 |

| | | | |
|----|-----|-----|-----|
| 24 | 300 | 40 | 2.3 |
| 24 | 350 | 85 | 2.6 |
| 24 | 400 | 117 | 1.8 |

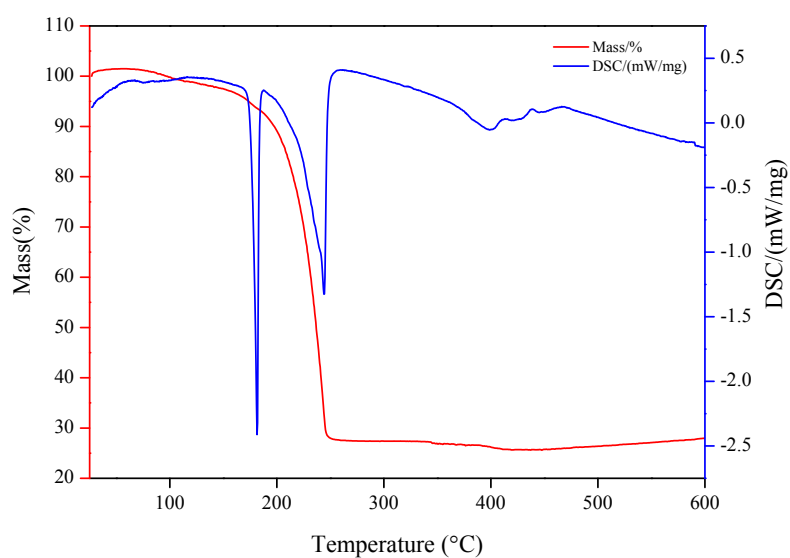


Figure S1. TGA/DSC curves for $[\text{Ni}(\text{dmamp}')_2]$.

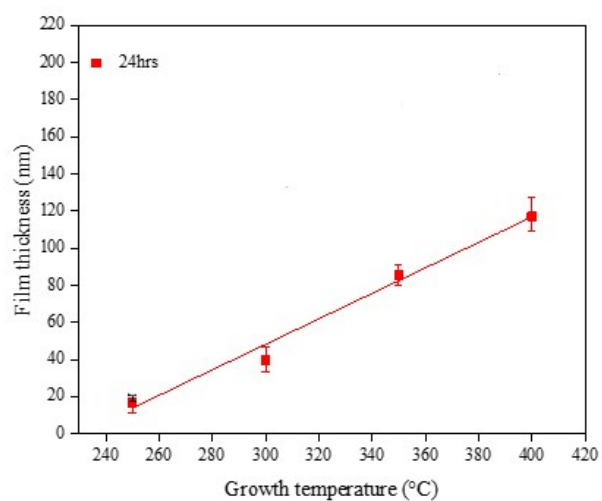


Figure S2: Temperature dependence on the film thickness of NiO films deposited by CVD of $[\text{Ni}(\text{dmamp}')_2]$ grown for a given time of 24 hours.

Films deposited at a growth temperature of 400 °C appeared visually non-uniform in thickness, with the inlet end of the substrate thicker than the outlet end of the substrate. Reduction of the growth temperature from 400 °C to 300 °C resulted in visually more uniform thin films with refractive index values more consistent with literature values for NiO. As a growth temperature of 300 °C appeared to provide visually uniform films with low roughness, subsequently the relationship between deposition time and NiO film thickness was investigated at this temperature (**Figure S3**).

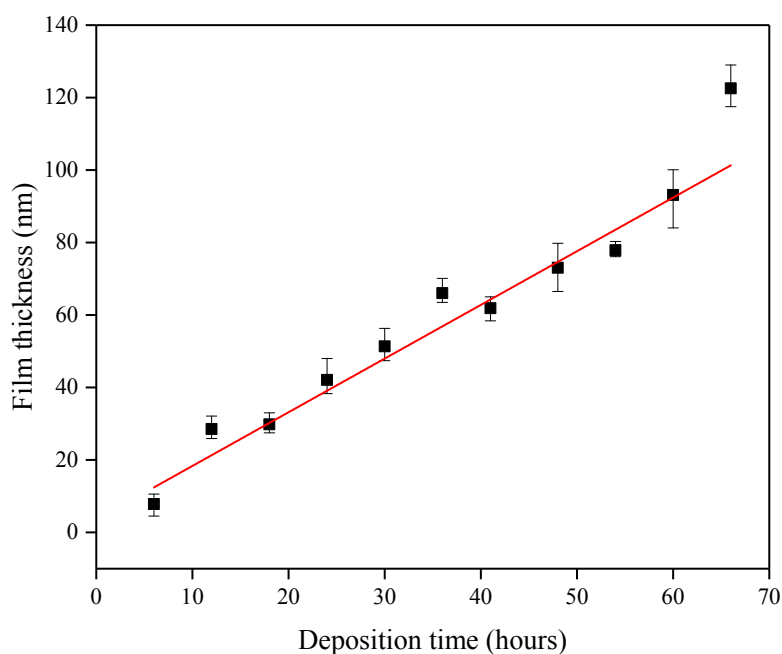


Figure S3: Relationship between deposition time and film thickness for NiO films deposited by CVD of $[\text{Ni}(\text{dmamp}')_2]$ at a single growth temperature of 300 °C.

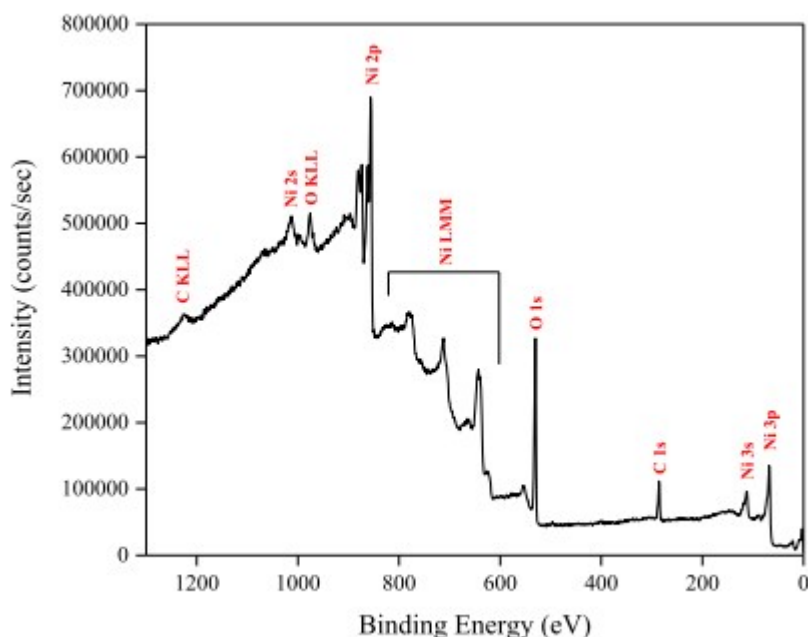


Figure S4: Typical XPS survey spectrum of NiO films deposited by CVD of $[\text{Ni}(\text{dmamp}')_2]$ at a growth temperature of 300 °C.

High resolution surface scans (Figure S5a) of the Ni2p peak confirm the presence of Ni^{2+} , with $2p_{3/2}$ and $2p_{1/2}$ peak binding energies of 855.4 eV and 873.2 eV respectively, with a peak separation of 17.8 eV. These values are within ± 0.2 eV of literature values.^[1] Characteristic satellite peaks for the $2p_{3/2}$ and $2p_{1/2}$ peaks were observed at 861.8 ± 0.2 eV and 880.2 ± 0.2 eV respectively. The prominent satellite shoulder 1.8 eV above the Ni $2p_{3/2}$ principal peak is unique to NiO.^[2]

De-convolution of the O1s peak reveals 2 peaks. The two peaks at higher binding energy, 532.8 ± 0.2 eV and 531.4 ± 0.2 eV can be attributed to surface bound carbon and surface adsorbed water, respectively. The peak with the lowest binding energy (529.6 ± 0.2 eV) is attributed to the O1s core peak of O^{2-} bound to Ni^{2+} (Figure S5b). Again, these peaks are consistent with literature values for these peak environments.

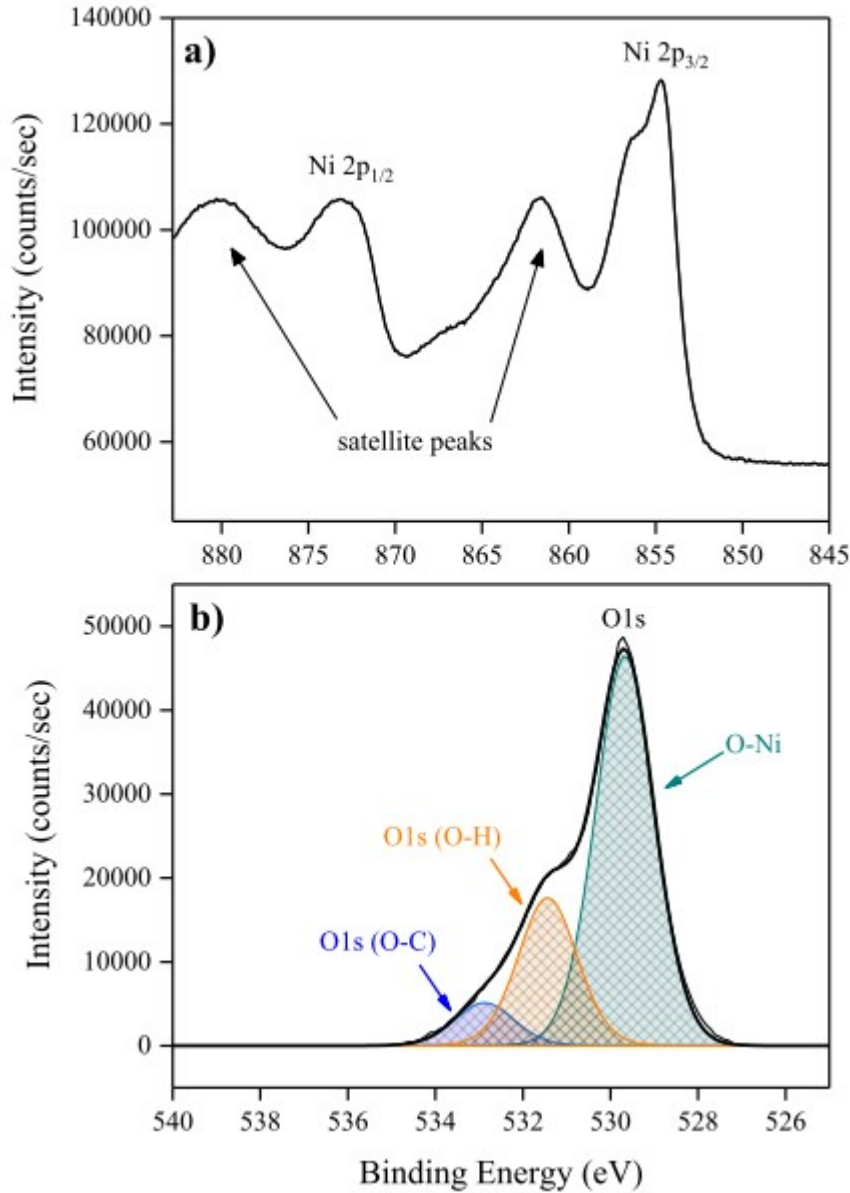


Figure S5: Typical high resolution surface XPS spectra of a) Ni2p peak and b) de-convoluted O1s peak for NiO films deposited by CVD of [Ni(dmamp⁺)₂] at a growth temperature of 300 °C.

Table S4: photovoltaic parameters for NiO control and NiO CVD devices.

| Photoelectrode | J_{SC} (mA cm ⁻²) | V_{OC} (V) | FF | PCE (%) |
|----------------|---------------------------------|------------------|-----------------|----------------|
| NiO Control | 21.3 (+/- 0.1) | 1.04 (+/- 0.001) | 0.66 (+/- 0.05) | 14.1 (+/- 0.1) |
| NiO CVD | 7.8 (+/- 0.5) | 1.02 (+/- 0.01) | 0.50 (+/- 0.5) | 3.9 (+/- 0.2) |

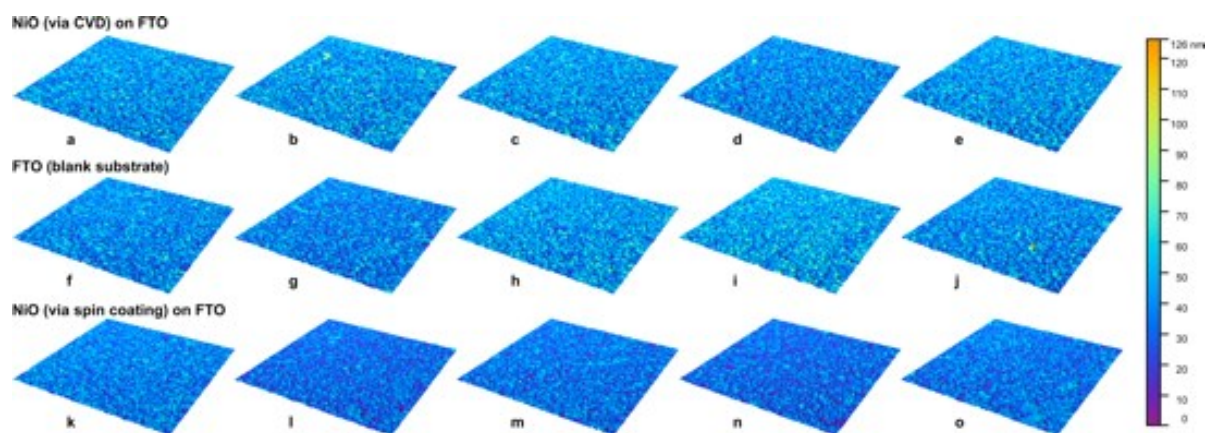


Figure S6: AFM images of 5x5 μm areas over a lateral resolution of 10 nm for five duplicate samples of FTO, CVD-deposited NiO/FTO and spin-coating-deposited NiO/FTO.

Table S5: AFM data of 5x5 μm areas over a lateral resolution of 10 nm for five duplicate samples of FTO, CVD-deposited NiO/FTO and spin-coating-deposited NiO/FTO.

| Aggregated (Mean) | | | |
|--|---------------------|---------------------------|-------------------------------|
| Sample | Z range (nm) | Average value (nm) | RMS roughness (Sq, nm) |
| FTO blank substrate | 97 | 42 | 11 |
| NiO (via CVD) on FTO | 100 | 43 | 12 |
| NiO (via spin.) on FTO | 73 | 35 | 9.7 |
| | | | |
| Aggregated (Standard Deviation) | | | |
| Sample | Z range (nm) | Average value (nm) | RMS roughness (Sq, nm) |
| FTO blank substrate | 17 | 3.4 | 0.24 |
| NiO (via CVD) on FTO | 10 | 1.6 | 0.47 |
| NiO (via spin.) on FTO | 2.9 | 2.5 | 0.13 |

^1H NMR and $^{13}\text{C}\{^1\text{H}\}$ NMR spectra for $[\text{Ni}(\text{dmamp}')_2]$ are shown in Figure S7 and Figure S8 respectively. The ^1H NMR spectrum shows 3 singlet proton environments at 1.19 ppm, 2.20 ppm and 2.97 ppm, corresponding to 4 methyl groups on the ligand backbone (Ha), 4 methyl groups on the nitrogen atoms (Hb) and 2 ethyl groups on the ligand backbone (Hc), respectively. The carbon NMR spectrum again shows 4 different peak environments at 19.7, 40.6, 67.9 and 75.8 ppm, which are associated to the carbon environments C1, C2, C3 and C4, respectively as shown in Figure S8.

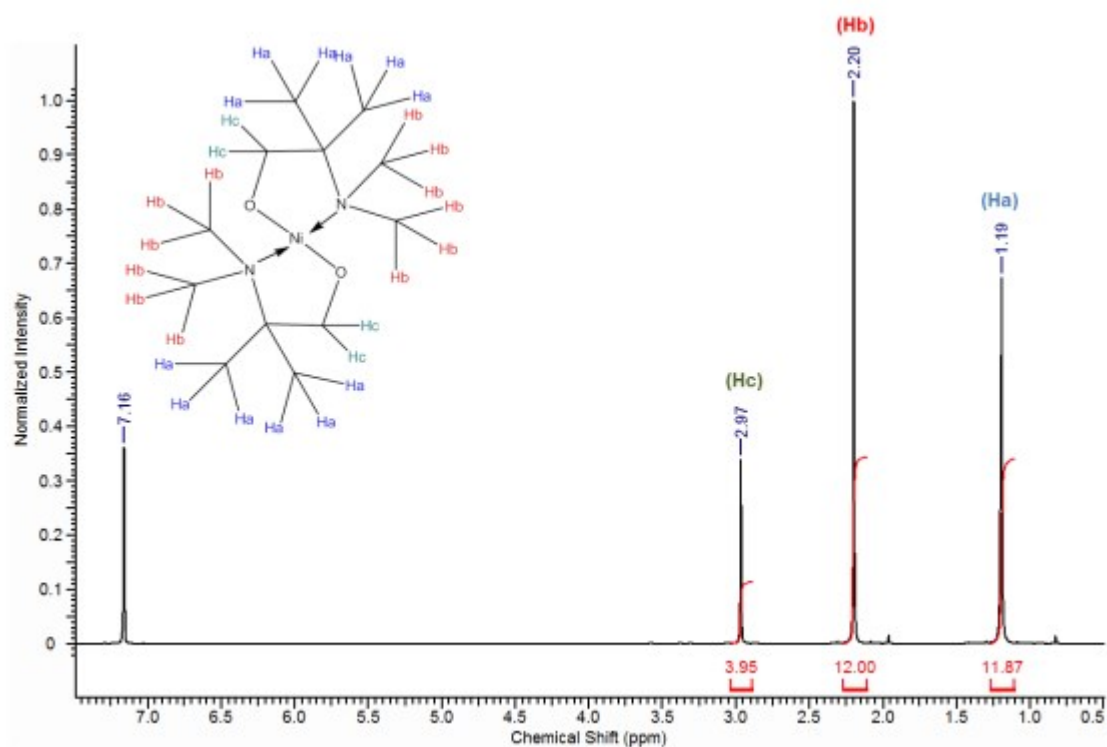


Figure S7: ¹H NMR spectrum of [Ni(dmamp')₂]

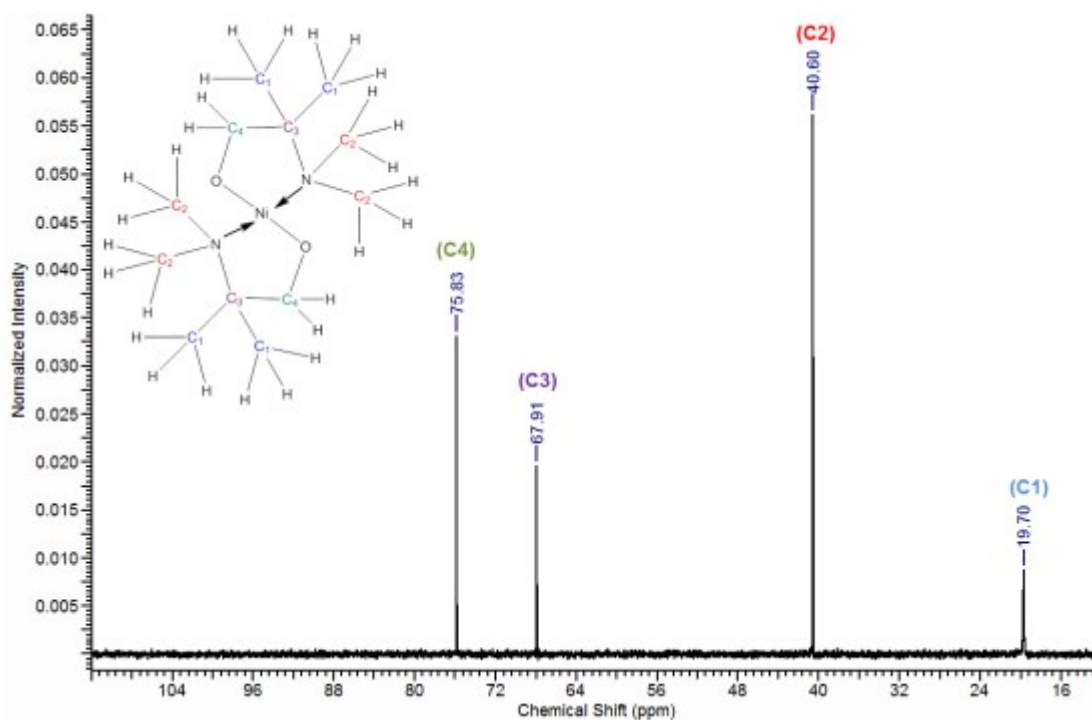


Figure S8: ¹³C NMR spectrum of [Ni(dmamp')₂]

References:

1. K.-C. Min, M. Kim, Y.-H. You, S. S. Lee, Y. K. Lee, T.-M. Chung, C. G. Kim, J.-H. Hwang, K.-S. An, N.-S. Lee, Y. Kim, *Surf. Coatings Technol.*, 2007, **201(22-23)**, 9252-9255.

2. N. S. McIntyre, M. G. Cook, *Anal. Chem.*, 1975, **47(13)**, 2208-2213.